# Integrity monitoring in Precise Point Positioning

Garrett Seepersad and Sunil Bisnath, *York University, Toronto, Canada*

## BIOGRAPHY

Garrett Seepersad is a Ph.D. candidate at York University, Toronto, Canada, in the Department of Earth and Space Science and Engineering. He has completed his honours B.Sc. in Geomatics at the University of West Indies and his M.Sc. in Geomatics Engineering at York University. His area of research currently focuses on the development and testing of PPP functional, stochastic and error mitigation models.

Dr. Sunil Bisnath is an Associate Professor in the Department of Earth and Space Science and Engineering at York University in Toronto, Canada. His research interests include geodesy and precise GNSS positioning and navigation.

## ABSTRACT

While much research effort has been applied to improving the accuracy of GPS Precise Point Positioning (PPP) coordinate solutions and reducing the duration of data collection needed to achieve such accuracies, little work has been published on the integrity of PPP solutions. Integrity and monitoring are essential components of any positioning / navigation system. In PPP processing, some parameters are estimated, modelled or eliminated without referring to any nearby reference stations. Thus providing integrity information for PPP single receiver estimates is all that more important. In the presented work, post-fit residuals, processing filter convergence, parameter estimation covariance and the solution position error are examined as PPP integrity indicators.

Through the implementation of one Receiver Autonomous Integrity Monitoring (RAIM) algorithm variant, a more rigorous PPP residual testing methodology was introduced rather than the conventional, empirical-based fixed outlier threshold method. With RAIM implemented, no significant improvements in positioning accuracy were noted during initialization; however, the algorithm is recommended for integration into PPP software as it offers an improved integrity monitoring system. Also presented is an overview of different methods to define initial convergence period in PPP. These methods include: 1) required convergence period based on the application; 2) a steady state definition; and 3) the proposed real-time PPP convergence indicator which notifies the user when the solution attains a steady state based on a user-defined accuracy threshold. The internal position uncertainty is the main indicator of the solution accuracy in PPP, as a reference solution may not always be available. The position uncertainty for the horizontal and vertical components were strongly correlated with the average position error with a correlation coefficient of 0.9. Finally, the most obvious navigation system requirement is the accuracy of the solution. In static mode, GPS PPP float solutions has an average accuracy of 7 and 13 mm in the horizontal and vertical components, respectively, with 24 hours of data processed.

## INTRODUCTION

The GPS (and now GNSS) PPP data processing technique has developed over the past 15 years to become a standard method for growing categories of positioning and navigation applications. These categories include but are not limited to crustal deformation monitoring, near real-time GPS meteorology, precise orbit determination of low Earth orbiting satellites and precise positioning of mobile objects. The main commercial applications of PPP are in the agricultural industry for precision farming, marine applications for sensor positioning in support of seafloor mapping and marine construction, and airborne mapping, for photogrammetric sensor positioning.

While much research effort has been applied to improving the accuracy of PPP coordinate solutions and the duration of data collection needed to achieve such accuracies, little work has been published on the integrity of PPP solutions. Integrity is the measure of the trust that can be placed in the information supplied by a navigation system (Ochieng et al. 2003). It includes the ability of the system to provide timely warnings to users when the system should not be used for navigation. Given that in PPP processing all parameters have to be accounted for, without multiple solutions as is in the case with double-differenced static, multi-baseline networks and network RTK, providing integrity information for PPP single receiver estimates is all that more important. The research presented describes integrity by internally determining realistic measurements of solution precision and also by internally detecting and removing of outlier measurements. It is important to have integrity monitoring during data processing as this is the only time when all the information used to form the position solution is present for in depth analysis. In the presented work, PPP integrity indicators include post-fit residuals, processing filter convergence, parameter estimation covariance, and solution position error. Each is discussed and developed as a means of providing integrity to the PPP solutions.

## PPP INTEGRITY INDICATORS

Presented are the different integrity indicators that have been identified and how they are used in PPP. Each shall be expanded in greater detail in the subsequent sections.

### The post-fit residuals

In least-squares filtering, the post-fit residuals are a measure of the quality of fit between the observed quantities and the estimated quantities. They can also be thought of as a measure of the appropriateness of the mathematical model used for the data (Anderson and Mikhail, 1998).

Residual testing in general assumes that errors in the observations and the residuals are normally distributed (Tiberius et al. 1999). Hence, before statistical tests can be applied it may be necessary to test that the residuals are normally distributed. The familiar bell-shape of the Normal Distribution frequency curve indicates that relatively large residuals can be expected, although these should occur much less frequently than relatively small residuals (Harvey et al. 1998; Rizos, 1997).

For example, 99.7% one dimension ($3\sigma$) of all residuals should be less than $\pm 3$ times the precision of the observable. Thus the probability of a residual exceeding $3\sigma$ is very small. If one or more of the residuals are significantly larger than either the other residuals in the set, or the residuals obtained from similar adjustments in the past, then it must be decided whether the anomalous observation represents an observation at the extremity of the Normal Distribution, in which case it should be retained, or it is indicative of an observation containing a gross error (or blunder), known as an "outlier", in which case it should be rejected (Harvey, 1998; Rizos, 1997).

As described by Rizos (1997) a typical “rule of thumb” in detecting outliers is to reject any observation with a residual exceeding three times the standard deviation of the observations. The current standard method for rejecting residuals is based on this ad hoc or empirically set value for rejecting the maximum pseudorange and carrier-phase post-fit residual. For example, in the CSRS-PPP code from NRCan (2011), if a carrier-phase residual is greater than 4.47 cm, the measurement for the respective satellite is rejected and the epoch is reprocessed, and if a pseudorange residual is greater than 4.47 m, the epoch is not reprocessed, but the satellite is rejected for the following epoch.

### Convergence

The use of PPP presents advantages for many applications in terms of operational flexibility and cost-effectiveness. One major limitations though is its relatively long initialization time as carrier-phase ambiguities converge to constant values and the solution reaches its optimal precision. PPP convergence depends on a number of factors such as the number and geometry of visible satellites, user environment and dynamics, observation quality, and sampling rate. As these different factors interplay, the period of time required for the solution to reach a pre-defined precision level will vary (Bisnath and Gao, 2009). PPP with ambiguity resolution (PPP-AR) would accelerate the overall solution convergence to give cm-level horizontal accuracy after 1 hour or less. The results presented by Collins et al. (2010) show after 1 hour 90% of the solutions approach 2 cm horizontal error, compared to 10 cm for the float PPP solution.

To address the issue of the user being aware of if the solution has truly converged, different methods to define initial convergence period in PPP shall be discussed and tested in greater detail. These methods include: 1) required convergence period based on the application; 2) a steady state definition; and 3) the proposed real-time PPP convergence indicator which notifies the user when the solution attains a steady state based on a user-defined accuracy threshold.

### Position uncertainty

The weighting of the observations are based on the covariance matrix of the observations, which through the functional model also plays a crucial role in the estimation of the covariance of the parameters. The covariance matrix of the position parameters, also known as the position uncertainty will be discussed and assessed in greater detail to determine its reliability to the PPP user. In most cases, the PPP user has no reference solution available. There have been very few studies that address this aspect of integrity monitoring in PPP to answer the questions: How accurate is my epoch PPP position? And, how realistic is the internal PPP uncertainty estimate? What we are actually asking is how the pseudorange and carrier-phase measurement as well as the modelled errors affect the estimated parameters (Langley, 1999).

The position uncertainty is given by the covariance matrix of the parameter estimates $C_{\hat{x}}$ in Equation 1. Where P represents the weights of the pseudorange and carrier-phase measurements, $P_{\hat{x}}$ is the a priori weighted constraints and A is the design matrix. The square root of the diagonal elements of $C_{\hat{x}}$ are the uncertainties of the estimated receiver coordinates, receiver clock-offset, wet component of the tropospheric delay and the corresponding uncertainties of the ambiguities.

$$C_{\hat{x}} = ( A^T P A + P_{\hat{x}})^{-1} \quad (1)$$

In GPS-related studies, for example, we might use Equation 1 to answer a variety of questions: What is the behaviour of the estimated parameter covariance matrix as a function of a particular satellite configuration? How do various model errors propagate into the receiver do coordinates as a function of satellite configuration? What is the tolerance value that a particular model error should not exceed to achieve a desired positioning accuracy?

**Position error**

Perhaps the most obvious navigation system requirement, position error, describes how well an estimated value agrees with a reference value. Ideally, the reference value should be the “true value” - some agreed-upon standard value. The expected accuracy of PPP is a function of the quality of the satellite orbits and clocks, observables and the quality of the error models used. The precise IGS final GPS satellite orbits and clocks have an accuracy of ~2.5 cm and ~75 ps respectively (IGS, 2013). Presented in Table 1 is a summary of all major corrections accounted for and the applied mitigative strategy. A dual-frequency GNSS receiver is typically used to mitigate the first-order effect of ionospheric refraction. A filtered linear combination of the dual-frequency pseudorange and carrier phase measurements will reduce the error effects on the range from 10s of metres to as little as a few millimetres in time. For the tropospheric refraction, the dry component is modelled and the wet component is estimated along with user position and ambiguity terms, resulting in a few millimetre residual error. To achieve the highest PPP positioning accuracy, error sources such as tidal loading, phase wind-up, and antenna phase offset and variation at the satellite and receiver are modelled. Residual terms such as pseudorange and carrier phase multipath and noise are typically filtered, stochastically de-weighted or simply ignored (Seepersad and Bisnath, 2013).

| Effect | Magnitude | Domain | Mitigation method | Residual error |
|---|---|---|---|---|
| Ionosphere | 10s m | range | linear combination | few mm |
| Troposphere | few m | range | modelling; estimation | few mm |
| Relativistic | 10 m | range | modelling | mm |
| Sat phase centre; variation | m - cm | pos; range | modelling | mm |
| Code multipath; noise | 1 m | range | filtering | 10s cm - mm |
| Solid Earth tide | 20 cm | position | modelling | mm |
| Phase wind-up (iono-free) | 10 cm | range | modelling | mm |
| Ocean loading | 5 cm | position | modelling | mm |
| Satellite orbits; clocks | few cm | pos; range | filtering | cm - mm |
| Phase multipath; noise | 1 cm | range | filtering | cm - mm |
| Rcv phase centre; variation | cm - mm | pos; range | modelling | mm |

**Table 1. Summary of error sources in PPP and mitigative strategy (Seepersad and Bisnath, 2013)**

**RECEIVER AUTONOMOUS INTEGRITY MONITORING (RAIM)**

RAIM is a receiver-internal technique designed to assess the integrity of GPS signals and plays a significant role in safety-critical GPS applications (Irsigler, 2008). There are many possible errors which affects the user, these include: excessive multipath, receiver error, and localized ionosphere or troposphere effects. RAIM is easily implemented and requires no additional hardware (Walter and Enge 1995), and it was originally designed to be incorporated as part of a standard point positioning processor for data collected by a code-only receiver. In cases where there are greater than 5 satellites tracked, post-fit residual analysis of the measurements allows for consistency amongst the observations, thus improvement of the overall solution integrity.

Through the adaptation of one RAIM algorithm variant, a PPP residual testing methodology is introduced here, which is more rigorous than the typical methods using empirically determined outlier tolerances. The algorithm was modified to be implemented within the PPP software as it offers increased integrity monitoring analysis of the residuals taking into consideration the number of satellites and geometry for each epoch, potentially allowing for improved solution initialization, resulting in potentially reduced convergence period. This independently-developed, modified RAIM routine is similar to those developed by Jokinen et al. (2011) and Merino and Laínez (2012).

### Fault Detection and Exclusion (FOE)

This section relates to the adoption of the code based RAIM, used for post-fit residuals outlier detection which has been modified for the code and phase filtering in PPP. There are several possible RAIM implementations which can be divided into methods for Fault Detection (FO) and Fault Detection and Exclusion (FOE). The Least-squares Residual Method is an example of FOE, as it is able to identify the affected signal and exclude it from navigation processing. The proposed standard RAIM scheme as discussed by Brown (1992) is based on a unified theory that says “under the condition of equal alarm rates, the least-squares-residuals, parity, and range-comparison RAIM methods all yield identical results”. The Least-squares Residual Method was modified here to fit the sequential least-squares model used within the York-PPP software by expanding from code only to code and phase measurements as well as including the a priori weighted constraints ($P_{\hat{x}}$).

The least-squares solution is used to calculate the residuals of the 2N measurements, where N is the number of satellites observed. This process is the linear transformation of the range measurement errors into the resulting residuals (Kuusniemi, 2007) given in Equation 2. The vector $\hat{e}$ has the dimension 2N x 1 and is the measurement error vector due to usual receiver noise, anomalies in propagation, imprecise knowledge of satellite position, satellite clock error and unexpected errors due to satellite malfunctions (Kuusniemi, 2007; Kouba and Héroux, 2001).

$$\hat{e} = (\mathrm{I} - \mathrm{A}(\mathrm{A}^{\mathrm{T}}\mathrm{PA} + \mathrm{P}_{\hat{x}})\mathrm{A}^{\mathrm{T}}\mathrm{P})\mathrm{W} \quad (2)$$

The sum of the squares of the residuals plays the role of the basic observable in the Least-squares Residual Method and is called the SSE in the equation below (Brown, 1992).

$$\mathrm{SSE} = \hat{e}^{\mathrm{T}}\hat{e} \quad (3)$$

Brown (1992) states that it is more convenient to use T as a test statistic, the quantity that is outlined in Equation 4, rather than SSE, as it is a function of both SSE and the number of satellites available, where N is the number of satellites and U is the number of unknowns.

$$\mathrm{T} = \sqrt{\frac{\mathrm{SSE}}{\mathrm{N-U}}} \quad (4)$$

The proposed standard scheme involves the formation of a simple scalar test statistic from the redundant measurements. This statistic is then compared with a pre-computed threshold (Td) (Sturza and Brown, 1990).

$$Td = \sigma^2 Q^{-1}(P_{FA}|N-U) \quad (5)$$

where:

$Q^{-1}(P_{FA}|N-U)$ - inverse chi-square probability function

$P_{FA}$ - maximum allowable false alarm rate

$\sigma$ - realistic noise

RAIM provides rigorous analysis of the post-fit residuals which may assist in detecting outliers residual, which may have been previously overlooked by standard PPP residual rejection. The threshold used in RAIM is dynamic, taking into account satellite variability. The typical standard method for rejecting residuals is based on ad hoc or empirically set values for rejecting the maximum pseudorange and carrier-phase post-fit residual. For example, in the CSRS-PPP code from NRCan (2011), if the carrier-phase residual is greater than 4.47 cm, the measurement for the respective satellite is reject and the epoch is reprocessed, and if the pseudorange residual is greater than 4.47 m the epoch is not reprocessed, but the satellite is rejected for the following epoch.

Illustrated in Figures 1 and 2 are examples of carrier phase residual rejection using the fixed threshold and RAIM based threshold, respectively. It can be seen in Figure 2 that the RAIM-based threshold dynamically takes into account varying satellite geometry and the number of satellites. Limited improvements were noted as datasets examined in this study were a subset of those used by the IGS for satellite clock and orbit determination. As such these stations use geodetic receivers which are positioned in clear open skies. Expected improvements should be noted in harsher environments such as urban canyons.

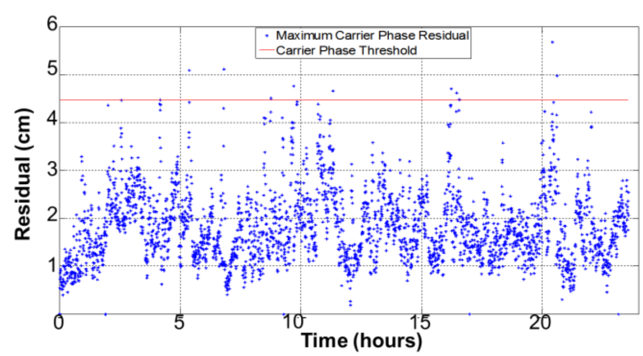


**Figure 1: Fixed threshold for carrier-phase residual rejection**

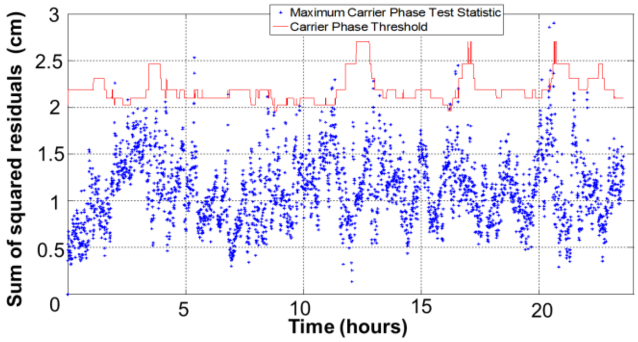


**Figure 2: RAIM based for carrier-phase residual rejection**

### Horizontal Protection Level

Horizontal Protection Level (HPL) was designed and is used for GNSS-equipped aircraft. It represents the radius of a circle in the horizontal plane with its centre being at the true position, which describes the region that is assured to contain the indicated horizontal position (FAA, 2011). Presented in this section is a modified version of HPL, adapted for implementation into the PPP software to be used as a real-time convergence indicator.

HPL is a function of the visible GPS satellites, user geometry, and expected error characteristics. The goal of an integrity algorithm is to provide a position solution within HPL. If the position integrity cannot be guaranteed to be protected within HPL with the given probabilities, the user will be notified and the position for that epoch will be rejected. Thus HPL is a very important part of an integrity method. The performance of GPS RAIM algorithms is mainly measured by HPL. The purpose of HPL is to make use of horizontal position error and screen out bad satellite constellation geometry. Poor geometries are detected and excluded by comparing HPL to the horizontal alert limit (HAL). The HAL is the maximum horizontal position error allowable for a given navigation mode without an alert being raised.

The state update position parameters $\Delta x_{XYZ}$, which is defined in a 3D Cartesian coordinate system is converted to a local topocentric coordinate system, $\Delta x_{ENU}$. A position vector at $(\varphi, \lambda, h)$ given in the (X,Y,Z) system is used to transform the coordinates to the easting, northing and up (E,N,U) system through multiplication by the orthogonal transformation matrix F (Borre, 2009):

$$F = \begin{bmatrix} -\sin\lambda & \cos\lambda & 0 \\ -\sin\varphi\cos\lambda & -\sin\varphi\sin\lambda & \cos\varphi \\ \cos\varphi\cos\lambda & \cos\varphi\sin\lambda & \sin\varphi \end{bmatrix} \qquad (6)$$

For failure detection purposes, the satellite whose bias error causes the largest slope is the one that is the most difficult to detect (typically the lowest in horizon) and produces the largest error for a given test statistic. The method used to calculate the maximum slope is presented below (Brown, 1992; Borre, 2009). The matrix M0 calculated in Equation 7 is resized to take into consideration only the X,Y,Z parameters, which are transformed to E,N,U in Equation 8. The slope values are calculated for each satellite for the pseudorange and carrier-phase observables in Equation 9. The maximum slope value is used to calculate the HPL, Equation 10.

$$M0 = (A^T P A + P_{\hat{x}})^{-1} A^T P \qquad (7)$$

$$M = F * M0(:,1:3) \qquad (8)$$

$$\alpha(i) = \sqrt{\left(\frac{M_{1i}^2 + M_{2i}^2}{S_{ii}}\right)} \qquad (9)$$

$$\alpha_{max} = MAX[\alpha] \qquad (10)$$

$$\sigma_0 = \sqrt{\frac{\hat{e}^T P \hat{e}}{n-5}} \qquad (11)$$

The S matrix represents the corresponding covariance matrix of the residuals. n represents the number of measurements. The maximum slope value is scaled by $\sigma$ which represents the standard deviation of the pseudorange and carrier-phase measurements.

$$HPL = \alpha_{max} * \sigma_0 \qquad (12)$$

An example of the application of the modified HPL is presented in the following section. The user-defined accuracy threshold is set as the modified HAL to indicate to the user in real-time when convergence has been attained.

## CONVERGENCE INDICATOR

PPP has been accepted by the scientific community and industry as a high accuracy GNSS processing method but it is limited in its application due to its characteristic solution convergence period. For static receivers that have the ability to collect data for hours, convergence is not a major limitation. For other users where time is not a luxury, the user would require a tool or indicator to know when sufficient data has been collected. That is, how does the user know a solution has converged? Presented are different strategies currently utilized, as well as a novel recommendation to be incorporated in the PPP software. Data from 80 IGS stations observed during the days of 244 to 250 in 2011 with hourly reinitialization were used for the recommendation of minimum convergence time required for different pre-defined thresholds and to examine the modified HPL. Float solutions were generated in static mode using the York-PPP software developed from NRCan (2011) original source code.

**Pre-defined threshold**

Presented are a subset of different applications of PPP and the period required for the solution to converge to different horizontal accuracy specifications. Recommendations for the quantity of data to be logged are based on the time 95% of the solutions took to achieve the specified horizontal accuracy level for the above described dataset. It is important to note solution accuracy is dependent upon various factors including the number of satellites tracked, constellation geometry, observation time, ephemeris accuracy, ionospheric disturbance, multipath and ambiguity resolution. The sites chosen were a subset of those processed regularly by most IGS stations that uses geodetic receivers which are positioned in clear open skies.

For less stringent applications of PPP such as hydrographic surveying for Order 1 and 2 surveys, horizontal requirements are 100 cm for primary control and 50 cm for recording the location of isolated signals or objects (IHO, 2005). For horizontal thresholds 100 and 50 cm, minimum convergence time of 10 and 5 minutes are recommended, respectively. For precision farming, accuracy threshold typically range from 10 – 20 cm horizontal (Wang and Feng, 2009). For a 10 cm horizontal threshold approximately 50 minutes is recommended, whereas for 20 cm, 25 minutes was required. For geodetic positioning, accuracy requirements range from 0.1 - 0.2, 0.5 and 1 - 5 cm (FGDC, 1998). At 0.1 - 0.2 mm accuracy range a PPP solution cannot be guaranteed by PPP 95% of the time. For a 5, 1 and 0.5 cm horizontal accuracy level it's recommended a minimum of 60, 23 and 24 hours of data be logged. Geodetic positioning is the most stringent of the different applications thus the long convergence period. Presented in Table 2 below is a summary of the different horizontal accuracy specifications discussed and the minimum recommended convergence time when initialized in static mode for float only solutions. A more detailed review of application specific specifications with recommended minimum convergence time can be found in Seepersad (2012).

**Table 2: Horizontal accuracy requirement at 95% confidence and required convergence period in static mode (Seepersad, 2012)**

| Horizontal accuracy 2σ | Recommended convergence period |
|---|---|
| 100 cm | 5 minutes |
| 50 cm | 10 minutes |
| 20 cm | 35 minutes |
| 10 cm | 50 minutes |
| 5 cm | 60 minutes |
| 2 cm | 9 hours |
| 1 cm | 23 hours |
| 5 mm | 24 hours |
| 2 mm* | - |
| 1 mm* | - |

*- not applicable for PPP

**Steady state**

PPP convergence can also be defined as when the positioning time series reaches a steady state. It is important to analyze each solution returned by the processor for all time instants $t \geq t_0$, where $t_0$ represents the initial time when the PPP processing has begun. The PPP solution consists of two components: a transient response and a steady state response (Sinha, 2007), such that

$$y(t) = y_{tr}(t) + y_{ss}(t) \tag{13}$$

The transient response is present in the short period of time immediately after the PPP processing starts. If the solution convergence is asymptotically stable, the transient response disappears, which can be represented as

$$\lim_{t \to \infty} y_{tr}(t) = 0 \tag{14}$$

If the system is unstable, the transient response will exponentially increase in time and in most cases the PPP solution would be practically unusable. Even if the PPP solution is asymptotically stable, the transient response should be carefully monitored since some undesired phenomena such as a poorly modelled error source will introduce biases into the final solution. Assuming the system is asymptotically stable, as more data are processed the system response would be determined by its steady state component only. It is important that the steady state response values are as close to the reference solution (when available) as possible.

PPP is an example of the under-damped case, which is the most common case in control system applications. A magnified figure of the system step response for the under-damped case is presented in Figure 3. The most important transient response parameters are the rise time ($t_r$), peak time ($t_p$), overshoot (OS) and settling time ($t_s$). The rise time refers to the time required for the solution to change from a specified low value to a specified high value. In PPP, the low value is zero (the reference solution) and the high value is the peak or the maximum value at which the solution converges from. It is difficult to define a rise time in PPP as the range of which solutions converge from varies. In this example, the peak time occurred in the first minute, which represents the time the solution took for the response to reach the first peak of the overshoot. The overshoot has a value of 157 cm representing when the solution reaches a maximum value. The settling time is the time the solution enters a steady state. The settling time occurs after 23 minutes, entering into a steady state with sub-centimetre deviation about zero (Sinha, 2007).

The response of an asymptotically stable linear system is in the long run determined by its steady state component. During the initial time interval the transient response decays to zero. The system response is represented by the steady state component for the remainder of the time series with an rms of a few centimetres, which proportionally decreases with time (Sinha, 2007). In PPP, it is important to have the steady state as close as possible to the reference solution so that the so-called steady state errors, which represent the differences between the steady state of the PPP solution and reference solution, can be defined.

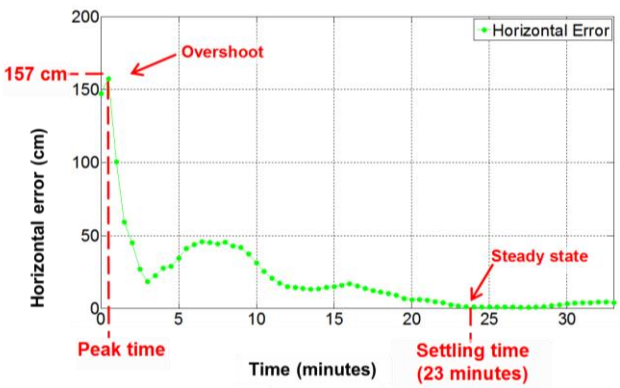


**Figure 3: Typical PPP convergence - an example of an under-damped system processed in static mode**

**Real-time convergence indicator**

Presented is a novel adaptation using the modified HPL as a dynamic indicator of when a steady state is achieved based on the user-defined accuracy specifications. Illustrated in Figure 4 is an example of the modified HPL and the state update for the horizontal position coordinates at the site ALBH for DOY 244 of 2012 processed in static mode. As expected, convergence is seen in both HPL and horizontal position update. The user's accuracy specifications is set to a radius of 2 cm to indicate to the user when a steady state is achieved. The user is notified in real-time when the radius of the HPL is less than or equal to 2 cm, which occurs after 23 minutes.

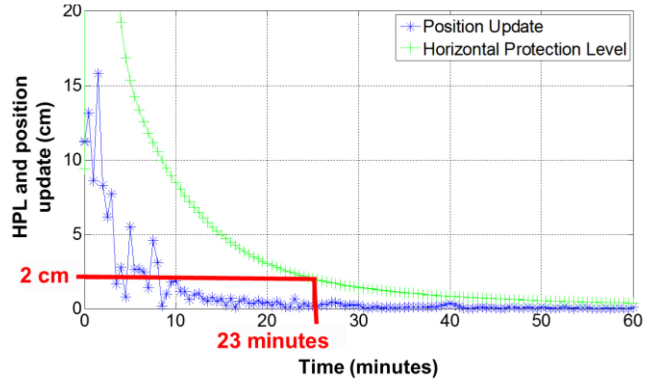


**Figure 4: Using HPL as a real-time indicator of PPP convergence**

Presented in Figure 5 are different user-defined accuracy specifications ranging from 1 to 5 cm and the time period required for datasets processed to achieve these specifications are achieved. The tighter user-defined specification, the higher the precision guaranteed to the user, but the longer convergence period required. At a 5 cm threshold, 95% of the data had an HPL radius of 5 cm or less at the 35 minute bin. The modified version of HPL is a good metric to define PPP convergence as it indicates to the user in real-time when a steady state is attained.

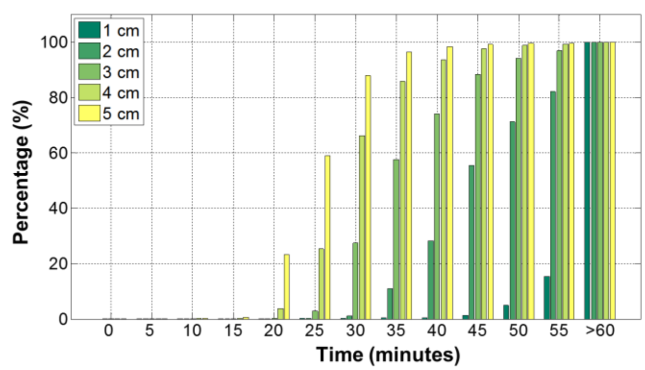


**Figure 5: Histogram showing time period taken to achieve different HPL threshold (Seepersad, 2012)**

**POSITION UNCERTAINITY**

Aside from measurement outlier detection, the covariance of the estimated position is the main indicator of the solution accuracy, as a reference solution may not always be available. An attempt to address the questions such as how accurate is my epoch PPP position? And how realistic is the internal PPP uncertainty estimate? An even larger sample dataset is examined, consisting of GPS data from 300 IGS stations observed during DOY 183 to 189 in 2012 were processed using the York-PPP software in static mode. The estimated float user position and associated uncertainty from the filter covariance are compared against the IGS weekly SINEX station estimates. Integrity was studied by examining the correlation between the determined PPP position error and the position uncertainty scaled to 95%.

The quality of the position uncertainty is defined by rigorous propagation of the observation uncertainties to the estimates of the unknowns. The observations are expected to be normally distributed and uncorrelated. In practice, due to the existence of biases and unknown and/or ignored correlation in the observations, they are not necessarily normally distributed potentially resulting in unrealistic state uncertainty estimates (Shirazian, 2013). For single point positioning, the position uncertainty is typically too optimistic. To ensure reliable position uncertainty is provided to the user, it is required that: 1) The stochastic model of the observations is well defined. The covariance matrix must be propagated with realistic observational variances and covariances. And 2) The systematic effects are completely removed (i.e., the functional model is correct) (Shirazian, 2013). GPS processing software, may use elevation dependent weights which may be a contributing factor to overly optimistic position uncertainties. Within the PPP code is a module which incooperates the uncertainties in the satellite orbits and clocks from their covariance matrix into the system of the observation equations. Such information will modify the covariance matrix potentially creating a more realistic position uncertainty.

Illustrated in Figures 6 and 7 are the correlation plots comparing the average position uncertainty and error for 300 stations in horizontal and vertical components, respectively. For each plot, the average position uncertainty and error of the 2010 datasets was taken for epochs at time 1, 5, 10, 15, 20, 25, 30 minutes, 1 to 6, 12, 18 and 24 hours. Both plots illustrate similar trends such as in the first hour, the average position uncertainty was overly pessimistic suggesting the error was worse than the true error for the horizontal and vertical components. For hours 2-6 and 12 a strong positive correlation is illustrated such that the average position uncertainty realistically depicts the magnitude of the average error in the horizontal and vertical components as the solution converged further. While at hours 18 and 24 the average position uncertainty and errors are correlated, the uncertainty becomes optimistic, suggesting the error is smaller than it actually is. The greatest outlier for both the horizontal and vertical components was after 30 minutes of processing. Overall, the position uncertainty for the horizontal and vertical components were strongly correlated with the position error with a correlation coefficient of 0.9.

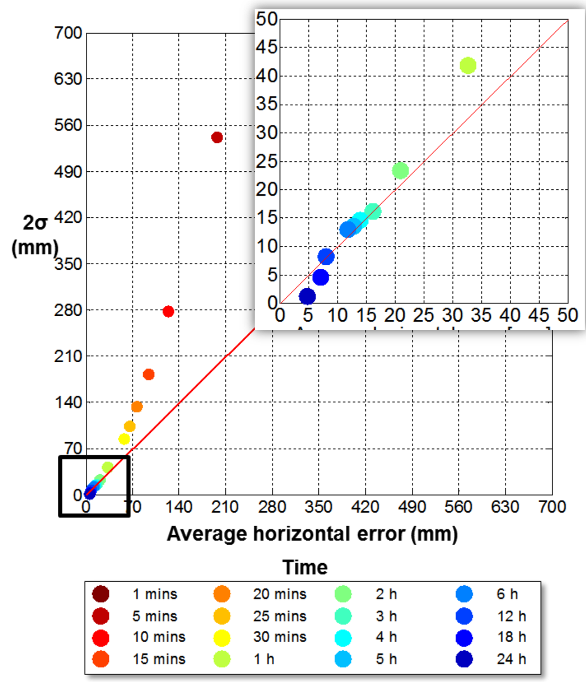


**Figure 6: Solution integrity for the horizontal component with a correlation coefficient of 0.9**

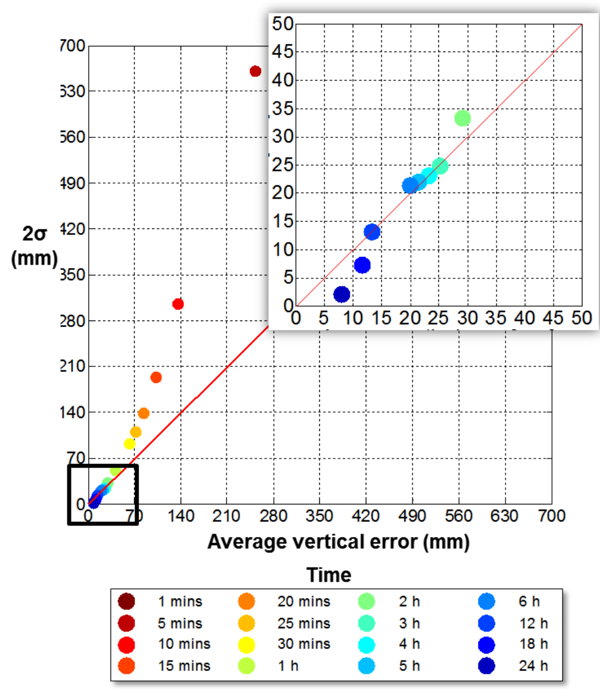


**Figure 7: Solution integrity for the vertical component with a correlation coefficient of 0.9**

## CURRENT ACCURACY OF PPP

Integrity indicators analysed thus far were all based on the internal information from the PPP filter. Quantification of the performance of PPP is an external examination of the integrity of PPP, this being the most critical navigation system requirement. To quantify the accuracy of PPP, the estimated positions were compared with the IGS weekly SINEX solution (CDDIS, 2013). The primary factors that affect the convergence period and the accuracy of PPP are the limited precision of current precise orbit and clock products and the effects of unmodelled error sources. Solution here refers to the solution generated after processing the entire 24 hour dataset. The distribution of the solutions in the horizontal and vertical components is illustrated in Figure 8 and Figure 9, respectively, with histogram bin sizes of 1 mm and 5 mm, respectively, for a sample size of 2010.

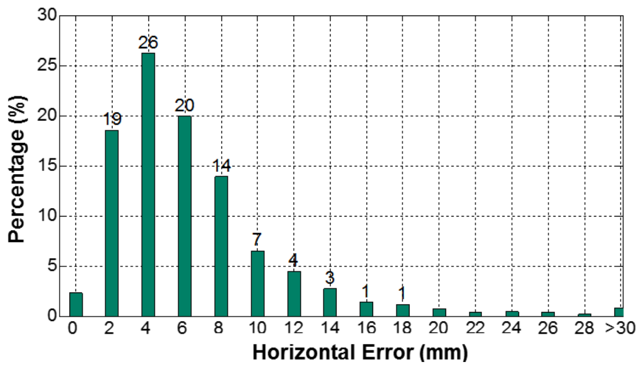


**Figure 8. Histogram showing absolute horizontal error**

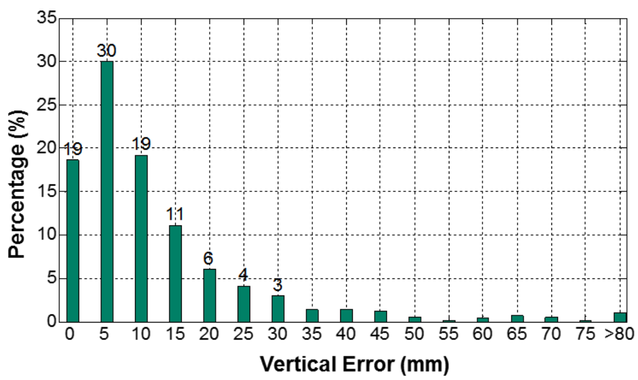


**Figure 9. Histogram showing absolute vertical error**

PPP is capable of producing sub-centimetre accuracy in the horizontal component and centimetre in the vertical. 99% of the data processed had an error in the horizontal component of less than or equal to 25 mm and 87% of the results had a horizontal error of less than one centimetre. In the vertical component, 99% of the data processed had an error of less than 80 mm and 95% of the results had an error less than 50 mm. It is expected for the vertical component to be of a lesser accuracy than that of the horizontal component due to satellite geometry (inherent to all modes of GNSS data processing) and the quality of the models used for atmospheric modelling and the solid Earth tides and ocean loading. A summary of the statistics of positions estimated are presented in Table 3. Overall, the solutions had an rms of 5, 6 and 13 mm in the north, east and up, respectively. No data were omitted in the statistical computation.

| Component | max | mean | std dev | rms |
|---|---|---|---|---|
| **Northing** | 27 | -1 | 5 | 5 |
| **Easting** | 26 | -1 | 6 | 6 |
| **Horizontal** | 28 | 1 | 7 | 7 |
| **Vertical** | 51 | -1 | 13 | 13 |
| **3D** | 52 | 2 | 15 | 15 |

**Table 3. Final solution produced by York-PPP from 24 hour datasets from 300 sites for DOY 183-189, processed in static mode for a total sample size of 2010. All units are in millimetres**

The horizontal component of the software was comparable to the results presented by Ge et al. (2008) with an rms 3 and 4 mm in north and east. In the up component, the rms was 1.7 times greater than published results by Ge et al. (2008). However, Ge et al. (2008) carried out a 7-parameter Helmert transformation when comparing their results against the SINEX coordinates. This questionable coordinate adjustment would most likely have further reduced the biases from their results, and may explain why the accuracy of their up component is smaller. The 7-parameter Helmert transformation between the two products allows the evaluation and removal of systematic differences caused by reference frame realizations that are slightly different (Mireault et al. 2008). This transformation is not required to be carried out as the solutions produced would have been in the same coordinate system as the IGS weekly satellite orbit and coordinate products.

Point positioning is calculated relative to a well-defined global reference system, in contrast to relative positioning, where the coordinates are in relation to some other fixed points. Eckl et al. (2001) describes the accuracy of static relative positioning with a geodetic-grade receiver is typically 5 mm + 0.5 ppm (rms) for the horizontal component and 5 mm + 1 ppm (rms) for the vertical component. This is the highest accuracy possible for static relative GPS positioning, as the fixed point would have an uncertainty associated with it. To determine if it is possible to replace static relative positioning by PPP, the inverse between PPP coordinates to determine static relative error statistics were calculated from the solution estimated by York-PPP and compared to the specifications published by Eckl et al. (2001). In the horizontal component the PPP solution had an accuracy of 7 mm, which is comparable to static relative positioning. In the vertical component, the accuracy of relative positioning is 2.6 times greater than that of the PPP solution.

## CONCLUSIONS AND RECOMMENDATIONS

Integrity is the measure of trust that can be placed in the information supplied by a navigation system. In PPP processing, some parameters are estimated, modelled or eliminated without referring to any nearby reference stations. This is why providing integrity information for PPP single receiver estimates is important. In the presented work, PPP integrity indicators include post-fit residuals, processing filter convergence, parameter estimation covariance and the solution position error.

**Post-fit residuals:** The post-fit residuals are a measure of the quality of fit between the observed quantities and the estimated quantities in the adjustment. The current standard method for rejecting residuals in PPP is based on an ad hoc or empirically set value for rejecting the maximum pseudorange and carrier-phase post-fit residual. The empirical value typically represents a threshold set to three times the standard deviation of the observations.

Through the implementation of one RAIM algorithm variant, a more rigorous PPP residual testing methodology was introduced rather than the typical use of empirically determined outlier tolerances. It was modified from code to a code and phase filter to be implemented within the PPP software because it offers increased integrity monitoring and analysis of the residuals. The RAIM algorithm takes into consideration the number of satellites and geometry for each epoch potentially allowing for improved solution initialization, resulting in potentially reduced convergence period. With RAIM implemented, no significant improvements in positioning accuracy were noted during initialization; however, the algorithm is recommended for integration into PPP software as it dynamically takes into account varying satellite geometry and the number of satellites thus offering an improved integrity monitoring system.

**Convergence:** PPP convergence depends on a number of factors such as the number and geometry of visible satellites, user environment and dynamics, observation quality and sampling rate. As these different factors interplay, the period of time required for the solution to reach a pre-defined precision level will vary. Presented were horizontal thresholds derived from various applications of PPP and minimum recommended convergence time required. It is important to note, that PPP convergence dependent upon various factors including the number of satellites tracked, constellation geometry, observation time, ephemeris accuracy, ionospheric disturbance, multipath and ambiguity resolution.

Also presented were different terms used in control systems that can be utilized in the analysis of PPP convergence. These terms included main transient response parameters such as the rise time, peak time, overshoot, settling time and steady state. The definition of a settling time and steady state in the context of PPP provided the foundation for a real-time convergence indicator of when a steady state has been attained based on a user-defined specification. The real-time convergence indicator is based on the application of the modified HPL as a dynamic indicator of when a steady state has been achieved based on the user-defined specification. The real-time convergence indicator allowed the user to be notified in real-time for data processing in static mode. The performance of the algorithm was examined against different thresholds for 1 week of data from 80 IGS stations with hourly reinitialization.

**Position uncertainty:** Aside from measurement outlier detection, the covariance of the estimated position is the main indicator of the solution accuracy in PPP, as a reference solution may not always be available. The estimated user position and associated uncertainty from the filter covariance are compared against the IGS weekly SINEX station estimates. Integrity was studied by examining the correlation between the determined PPP position error and the position uncertainty scaled to 95%.

Overall, the average position uncertainty for the horizontal and vertical components were strongly correlated with the average position error with a correlation coefficient of 0.9. During the first hour, the position uncertainty was pessimistic, suggesting the error was worse than the true error for the horizontal and vertical components. For hours 2-6 and 12 a strong positive correlation was illustrated such that the average position uncertainty realistically depicts the magnitude of the average error in the horizontal and vertical components. While at hours 18 and 24 the average position uncertainty and errors are correlated, the uncertainty becomes optimistic, suggesting the error is smaller than it actually is.

**Position error:** Perhaps the most obvious navigation system requirement, accuracy describes how well a measured value agrees with a reference value. Ideally, the reference value should be the “true value” - some agreed-upon standard value. The expected accuracy of PPP is a function of the quality of the satellite orbits and clocks, observables and the quality of the error models used in PPP. For a large sample size of 2010 datasets, processed in static mode using York-PPP, after 24 hours the float solution had an average accuracy of 7 and 13 mm in the horizontal and vertical components, respectively.

Future work would consist of reducing the computational load of the proposed modified RAIM algorithm by methods such as pre-computing the thresholds. Also, the position uncertainty from the PPP solution requires further analysis. While on average there is strong correlation, there are sites with weak correlation. Introducing a more realistic stochastic de-weighting scheme would also contribute to a more reliable position uncertainty. Also, further analysis of the satellite and clock position uncertainty currently used within stochastic de-weighting scheme of the conventional PPP software. Application of the techniques discussed would also be extended to multi-GNSS processing and PPP-AR.

**ACKNOWLEDGMENTS**

The research reported in this paper was funded in part by the Natural Sciences and Engineering Research Council of Canada. The results presented in this paper are derived from data and products provided by Natural Resources Canada, the International GNSS Service and Crustal Dynamics Data Information System.

**REFERENCES**

Anderson J, and Mikhail E (1998) *Surveying: Theory and Practice*, WCB/McGraw-Hill Boston, 1200 p.

Bisnath S, and Gao Y (2009) "Current State of Precise Point Positioning and Future Prospects and Limitations." *International Association of Geodesy Symposia – "Observing our Changing Earth"*, Vol.133 pp. 615-623.

Borre K (2009) "GPS EASY Suite II: Carrier Phase and Pseudorange." *Inside GNSS*, Vol. 4 No. 5, pp. 48-51.

Brown RG (1992) "A Baseline GPS RAIM Scheme and a Note on the Equivalence of Three RAIM Methods." *Navigation*, Vol. 39 No. 3, pp. 301-16.

CDDIS (2013) *Crustal Dynamics Data Information System.* ftp://cddis.gsfc.nasa.gov/pub/gps/ Accessed: 2013.

Collins P, Bisnath S, Lahaye F, and Héroux P (2010) "Undifferenced GPS Ambiguity Resolution using the Decoupled Clock Model and Ambiguity Datum Fixing." *Navigation*, Vol. 57 No. 2, pp. 123-35.

Eckl M, Snay R, Soler T, Cline M, and Mader G (2001) "Accuracy of GPS-Derived Relative Positions as a Function of Interstation Distance and Observing-Session Duration." *Journal of Geodesy*, Vol. 75 No. 12, pp. 633-40.

FAA (2011) "Wide-area Augmentation System Performance Analysis Report, Report #39." *Federal Aviation Administration.* http://www.nstb.tc.faa.gov/REPORTS/waaspan39.pdf Accessed: 2012.

FGDC (1998) "Geospatial Positioning Accuracy Standards - Part 2: Standards for Geodetic Networks." *The Federal Geographic Data Committee.* http://www.fgdc.gov/standards/projects/FGDC-standards-projects/accuracy/part2/chapter2 Accessed: 2012.

Ge M, Gendt G, Rothacher M, Shi C, and Liu J (2008) "Resolution of GPS Carrier-Phase Ambiguities in Precise Point Positioning (PPP) with Daily Observations." *Journal of Geodesy*, Vol. 82 No. 7, pp. 389-99.

Harvey BR, Elford D, and Turner C (1998) "Calculation of 3D Control Surveys." *Australian surveyor*, Vol. 43 No. 2, pp. 109-18.

IGS (2013) "IGS Products." *The International GNSS Service (IGS).* http://igscb.jpl.nasa.gov/components/prods.html Accessed: 2013.

IHO (2005) "Chapter 6: Topographic Surveying, in Manual on Hydrography." *International Federation of Surveyors.* http://www.fig.net/commission4/iho/M-13_Chapter_1_and_contents.pdf Accessed: 2013.

Irsigler, M (2008) *"Multipath Propagation, Mitigation and Monitoring in the Light of Galileo and the Modernized GPS."* Ph. D. dissertation, University of Federal Armed Forces Munich, Germany, 222 p.

Jokinen, A, S Feng, C Millner, W Schuster, W Ochieng, C Hide, and T Moore (2011) "Precise Point Positioning and Integrity Monitoring with GPS and GLONASS." *Royal Institute of Navigation.* http://www.rin.org.uk/Uploadedpdfs/ConferenceProceedings/Jokinen%20paper%202A-web.pdf Accessed: 2013.

Kouba J, and Héroux P (2001) "Precise Point Positioning using IGS Orbit and Clock Products." *GPS solutions*, Vol. 5 No. 2, pp. 12-28.

Kuusniemi, H (2007) "GNSS Solutions: Is fault detection/RAIM useful in areas of severe signal degradation, in such as urban environments?" *Inside GNSS.* http://www.insidegnss.com/auto/JulyAug07-GNSS-Sol.pdf Accessed: 2012.

Langley RB (1999) "The Integrity of GPS." *GPS World*, Vol. 10 No. 3, pp. 60-3.

Merino R, and Laínez M (2012) "Integrity for Advanced Precise Positioning Applications." *Proceedings of the 25th International Technical Meeting of The Satellite Division of the Institute of Navigation*, Nashville, TN, pp. 2742-2758.

Mireault Y, Tétreault P, Lahaye F, Héroux P, and Kouba J (2008) "Online Precise Point Positioning." *GPS World*, Vol. 19 No. 9, pp. 59-64.

NRCan (2011) "About Us." *Natural Resources Canada.* http://www.nrcan-rncan.gc.ca/com/index-eng.php Accessed: 2013.

Ochieng WY, Sauer K, Walsh D, Brodin G, Griffin S, and Denney M (2003) "GPS Integrity and Potential Impact on Aviation Safety." *Journal of Navigation,* Vol. 56 No. 1, pp. 51-65.

Rizos, C (1997) "Section 9.1.5: Outlier testing and residuals." *Principles and practice of GPS surveying.* http://www.gmat.unsw.edu.au/snap/gps/gps_survey/chap9/915.htm Accessed: 2013.

Seepersad G, and Bisnath S (2013) "Assessing the Accuracy of PPP." *Geomatica,* Vol. To be published.

Seepersad, G (2012) *"Reduction of Initial Convergence Period in GPS PPP Data Processing."* M. Sc. dissertation, York University, Toronto, Ontario, 131 p.

Shirazian, M (2013) *"Quality Description in GPS Precise Point Positioning."* Ph. D. dissertation, Royal Institute of Technology, Sweden, 133 p.

Sinha A (2007) *Linear Systems: Optimal and Robust Control,* 1st edn. CRC Press, 488 p.

Sturza MA, and Brown AK (1990) "Comparison of Fixed and Variable Threshold RAIM Algorithms." *Proceedings of the 3rd International Technical Meeting of the Satellite Division of The Institute of Navigation (ION GPS 1990),* pp. 437-443.

Tiberius C, Jonkman N, and Kenselaar F (1999) "The Stochastics of GPS Observables." *GPS World,* Vol. 10 No. 2, pp. 49-54.

Walter T, and Enge P (1995) "Weighted RAIM for Precision Approach." *Proceedings of the 8th International Technical Meeting of the Satellite Division of The Institute of Navigation (ION GPS 1995),* Palm Springs, CA, pp. 1995-2004.

Wang J, and Feng Y (2009) "Integrity Determination of RTK Solutions in Precision Farming Applications." *Proceedings of the Surveying and Spatial Sciences Institute Biennial International Conference 2009,* Surveying and Spatial Sciences Institute, pp. 1277-1291.